Physical Changes in the Patagonian Shelf

Martín Saraceno, Jacobo Martín, Diego Moreira, Juan Pablo Pisoni, and Mariano Hernán Tonini

Introduction

The coastal marine regions are expected to be the most vulnerable to the effects of climate change, such as variations in sea level, extreme events, and temperature changes, among others (IPCC 2014). Coastal ecosystems are already affected by the combination of these factors and by the adverse effects of human activities (Oppenheimer et al. 2019). The physical changes observed in the region that extends from the Médanos point (36.9°S) to Tierra del Fuego (55°S) and includes the waters from the coastline to the continental shelf-break are described in this chapter, with particular emphasis in the coastal area. The Patagonian shelf (Fig. 1) can be divided

M. Saraceno (✉) · D. Moreira
Centro de Investigaciones del Mar y la Atmósfera (CIMA-CONICET/UBA), Buenos Aires, Argentina

Departamento de Ciencias de la Atmósfera y de los Océanos, FCEN, Universidad de Buenos Aires, Buenos Aires, Argentina

Unidad Mixta Internacional-Instituto Franco-Argentino para el Estudio del Clima y sus Impactos (UMI-IFAECI/CNRS-CONICET-UBA-IRD), Buenos Aires, Argentina
e-mail: saraceno@cima.fcen.uba.ar

J. Martín
Centro Austral de Investigaciones Científicas (CADIC-CONICET), Ushuaia, Argentina

Instituto de Ciencias Polares, Ambiente y Recursos Naturales, Universidad Nacional de Tierra del Fuego, Ushuaia, Argentina

J. P. Pisoni
Centro para el Estudio de Sistemas Marinos (CESIMAR-CCT CENPAT-CONICET), Puerto Madryn, Argentina

Instituto Patagónico del Mar (IPaM, UNPSJB), Puerto Madryn, Argentina

M. H. Tonini
IPATEC (Instituto Andino-Patagónico de Tecnologías Biológicas y Geoambientales), CONICET/UNCO, S. C. de Bariloche, Argentina

E. W. Helbling et al. (eds.), *Global Change in Atlantic Coastal Patagonian Ecosystems*, Natural and Social Sciences of Patagonia, https://doi.org/10.1007/978-3-030-86676-1_3

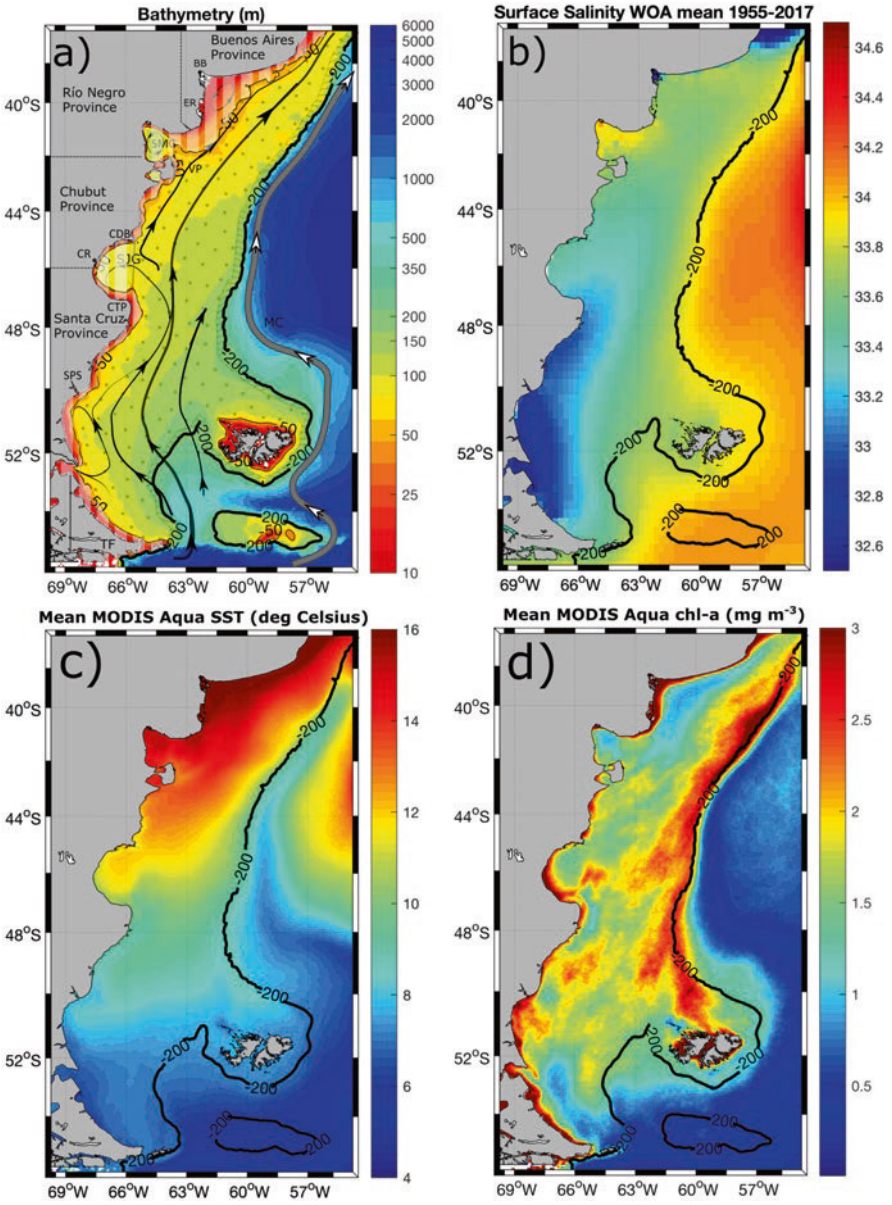

Fig. 1 (**a**) Bathymetry (GEBCO 2020); black thick and thin lines are the 200 m and 50 m isobaths; gray line with white arrows represents the northward Malvinas current; black arrows represent the mean surface circulation over the shelf adapted from Piola et al. (2018); (**b**) Surface salinity from World Ocean Atlas, data collected between 1955 and 2017; (**c**) mean MODIS Aqua SST (degree Celsius) for the period 2002–2020; (**d**) mean MODIS Aqua Chl *a* concentration (mg m^{-3}) for the period 2002–2020. *BB* Bahía Blanca estuary, *ER* El Rincón, *SMG* San Matías gulf, *VP* Valdés península, *CR* Comodoro Rivadavia, *SJG* San Jorge gulf, *CDB* Dos Bahías cape, *CTP* Tres Puntas cape, *MC* Malvinas current, *SPS* southern Patagonian shelf, and *TF* Tierra del Fuego

in three regions from the coast to the open ocean: we define here the inner shelf as the portion of the sea that goes from the coastline up to the 50 m isobath, including all the gulfs and channels; the outer shelf is considered as the 40 km fringe closest to the shelf-break and the middle shelf as the region included between the inner and the outer shelf regions. The inner shelf is characterized by distinct morphological, climatic, and oceanographic features. With more than 3000 km of coasts, the region encompasses four distinct subregions: Buenos Aires shelf, North Patagonian gulfs, San Jorge gulf, and the Southern Patagonian shelf (SPS). The SPS includes the Beagle channel and the Magellan strait. The chapter is organized as follows: data and methods are presented followed by the description of the middle and outer continental shelf, along with the analysis of the observed trends of sea surface temperature, chlorophyll *a* (hereafter Chl *a*), and sea level height. The four subregions are then described individually, followed by highlights of the more relevant results presented.

Data and Methods

To compute long-term physical changes in the ocean, long-term time series of observations are needed. In the Argentine continental shelf, the longest in situ records correspond to sea level observation made by tide gauges (Lanfredi et al. 1998; Santamaria-Aguilar et al. 2017). With data recorded since 1906, the Mar del Plata tide gauge is one of the longest time series of sea level in the world. Yet, apart from the tide gauges' measurements, no long (>10 years) time series are available in the continental shelf, as is mostly the case in the rest of the ocean. On the other hand, satellite altimetry missions offer reliable data of the surface of the ocean that, in some cases, can be longer than 20 years. In particular satellite altimetry represents very accurately sea surface height (SSH) in the region of study (Saraceno et al. 2010; Ruiz Etcheverry et al. 2015, 2016; Strub et al. 2015). Here we compute and analyze sea surface temperature (SST) and Chl *a* concentration for years 2002–2020 and of SSH for years 1993–2020.

In Situ Data

The mean sea surface salinity is retrieved from the World Ocean Atlas (Boyer et al. 2013). This atlas has been constructed with quality controlled in situ observations between 1955 and 2017.

Satellite Data

SST and Chl *a* were obtained from the Oceancolor website (https://oceancolor.gsfc.nasa.gov/, NASA 2018). We used the complete mission (June 2002–May 2020) of monthly maps with 4 km spatial resolution of the two variables. Monthly composites attenuate the instantaneous images but help decrease almost completely the absence of data due to cloudiness. SSH was obtained from Marine Copernicus website (https://resources.marine.copernicus.eu/). We used monthly values of mapped delayed time composites of multiple satellite altimetry missions (product number 008_047) for the period January 1993–December 2020. The spatial resolution of the SSH maps is ¼ of degree.

Numerical Model Output

The output simulations were performed using a numerical model called the Regional Ocean Modelling System (ROMS, Shchepetkin and McWilliams 2005). In the vertical, the primitive equations are discretized over variable topography using stretched terrain-following coordinates. In the horizontal, the primitive equations are evaluated using orthogonal curvilinear coordinates on a staggered Arakawa C-grid. For the vertical mixing parameterization, we selected the scheme developed by Mellor and Yamada (1982). The bathymetry is based on digitized nautical charts. The computational grid has three open boundaries (south, west, and north) where we imposed tidal amplitudes and phases of principal constituents of the region interpolated from a global tidal model (TPXO6, Egbert et al. 1994). We used here two different configurations: one for the north Patagonian gulf region and another for San Jorge gulf domain. For more details in model setup simulations (grid, forcings, open boundaries, etc.), see Tonini and Palma (2017) for the north Patagonian gulfs region and Palma et al. (2020) for San Jorge gulf domain. The rate of tidal energy dissipation was computed as in Tonini and Palma (2017) from the bottom currents field using a bottom drag coefficient of 0.003.

Data Processing

To compute SST and SSH trends, the best fit (in the least square sense) of the sum of annual and semiannual harmonic was subtracted to the original time series at each pixel. Filtering the seasonal cycle from Chl *a* time series is more difficult, as large intra-seasonal and intra-annual variability is present in this variable in the Patagonian shelf (Saraceno et al. 2005). Yet, every year the largest values are observed in the austral spring season (Saraceno et al. 2005; Romero et al. 2006; Andreo et al. 2016). We therefore averaged the monthly values of October, November, and December for every year and computed the trend of the resulting

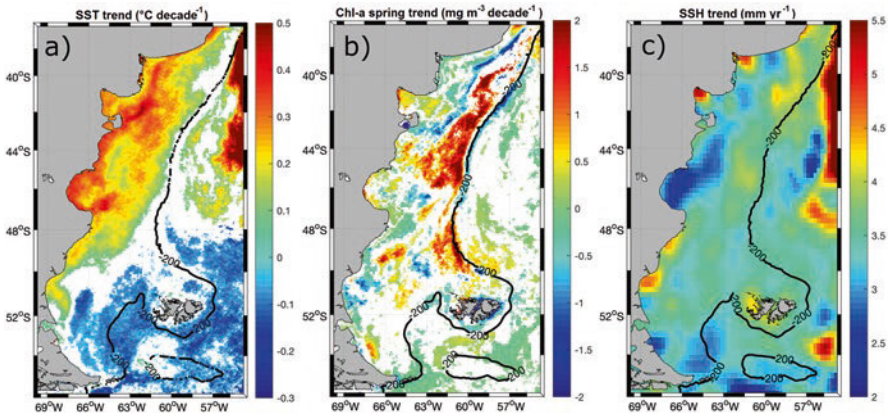

Fig. 2 (**a**) SST trend (°C decade^{-1}); (**b**) austral spring Chl *a* trend (mg m^{-3} decade^{-1}); (**c**) SSH trend (mm yr^{-1}). Both in SST and SSH, the seasonal cycle has been removed. White pixels correspond to nonsignificant (95% confidence level) values

time series at every pixel. The three trend maps obtained are displayed in Fig. 2. Nonsignificant values within the 95% confidence level according to the Student t-test are masked.

Middle and Outer Patagonian Shelf

Baseline

The middle and outer shelf is a wide plateau subject to intense westerly winds and high tidal variability. The outer shelf is bounded offshore by the cold, nutrient-rich, and relatively freshwaters coming from the Antarctic Circumpolar Current. The cold waters flow northward along the Patagonian slope, advected by the Malvinas Current (MC) to about 38°S, where the MC encounters the southward flowing Brazil current and diverges eastward. Both currents form the so-called Brazil/Malvinas Confluence region, through which most of the shelf waters are exported offshore (Franco et al. 2018). The MC is an important barrier for shelf waters (Beron-Vera et al. 2020), though significant intrusions along the shelf-break are observed (Piola et al. 2010). The bathymetry (Fig. 1a) shows that the continental shelf is limited by the 200 m isobath and has a very slow gradient from the coast to the shelf-break.

Continental shelf waters are characterized by relatively freshwaters as compared to the adjacent offshore waters (Fig. 1b). The two main sources of freshened waters are Pacific Ocean-diluted waters and estuarine waters from Río de la Plata. The former enters the Argentinian continental shelf through the Le Maire strait, the

southern Patagonian shelf-break and the Magellan strait (Guihou et al. 2020), and produces a particular signature in surface salinity as shelf waters are advected northward by the Patagonian current (Brandhorst et al. 1971). The dilution of the Pacific waters occurs mainly because of the excess of precipitation over the western flank of the southern Andes and due to the seasonal melting of glaciers in southern Patagonia. The second main source of freshwater, the Río de la Plata, drains an average of 22,000 $m^3\ s^{-1}$ at about 34.5°S through the widest estuary in southern South America. Most of the Río de la Plata outflow is advected northward to the Uruguay and southern Brazilian shelves forced by the dominant winds (Piola et al. 2005; Saraceno et al. 2014). Southwesterly winds can advect Río de la Plata freshwaters southward up to 38°S along the coast of the Buenos Aires province, particularly in austral summer (Piola et al. 2018). The combined discharge from all rivers along the Patagonian coast are an order of magnitude lower than the Río de la Plata input of freshwaters and have been reported to have only a local influence, as is discussed below. The unique distinctive source of waters saltier than the mid-shelf waters is the San Matías gulf (SMG) (Fig. 1b). As detailed in the North Patagonian Gulfs Section, SMG has a closed circulation in austral summer which, together with the fact that net evaporation is larger than precipitation during that season, makes the SMG an important source of saltier water. Saltier water produced in the SMG exits the gulf through the northern portion of the mouth and is advected toward the north over the continental shelf, mainly during austral autumn (Lucas et al. 2005; Tonini et al. 2013).

The mean SST (Fig. 1c) shows that the largest values are located close to the coast, along the Buenos Aires and Río Negro provinces and that a marked negative gradient toward the South is only interrupted by the signature of the MC. Indeed, the MC advects the cold sub-Antarctic waters up to about 40°S and clearly affects the SST along its path (Saraceno et al. 2004).

Finally, mean Chl *a* (Fig. 1d) shows that the largest values are observed along the upper portion of the Patagonian slope and adjacent outer shelf region as well as all along the coast. Chl *a* concentrations along the coast (Fig. 1d) might be associated with the stimulation of phytoplankton growth by the inflow of riverine nutrients but are also very likely biased by dissolved organic matter of terrestrial origin and resuspension caused by tidal mixing (see Villafañe et al. this volume).

The large values along the shelf-break and in the outermost portion of the continental shelf are sustained by the upwelling of the nutrient-rich MC waters over the upper portion of the slope. The mechanism responsible for such upwelling has not been proven yet, but several hypotheses based on observational evidence and numerical models have been proposed. The main hypotheses are the divergence of the MC (Matano and Palma 2008), the divergence produced by wind stress curl (Saraceno et al. 2005; Carranza et al. 2017) and the passage of coastal-trapped waves (Acha et al. 2004; Saraceno et al. 2005; Poli et al. 2020). In the mid-shelf, the largest Chl *a* concentrations are associated with tidal fronts (Acha et al. 2004; Romero et al. 2006).

Observed and Expected Changes

Figure 2a shows that SST marks a significant positive trend (up to 0.04 °C per year) north of ~50°S, while negative values (up to −0.02 °C per year) are observed south of 50°S. Similar results were observed in Leyba et al. (2019) using Reynolds et al. (2007) SST data for the period 1982–2015. Leyba et al. (2019) also highlighted that the SST trend in the region is strongly linked to trends in heat fluxes. The negative SST trend observed in the southern portion of the region is associated with the positive trend observed in the dominant westerly winds within those latitudes (Marshall 2003). Stronger westerlies favor the entrance of colder offshore waters via a larger Ekman transport. The spring Chl *a* linear trend observed in Fig. 2b shows values as large as 2 mg m^{-3} over a 10-year period in the outer portion of the continental shelf between 50 and 40°S. Marrari et al. (2017) produced a 20-year (1997–2017) time series merging SeaWiFS and MODIS Aqua data and analyzed the total Chl *a* trend around South America. They found an order of magnitude smaller values as compared to what is shown in Fig. 2b. However, results are not comparable because (i) we considered only austral spring months and Marrari et al. (2017) used all-year-round months and (ii) the period considered in the two studies is not the same. The mechanisms that might explain the large Chl *a* trends observed should be investigated.

The linear trend in SSH (Fig. 2c) ranges between 2 and 5 mm yr^{-1} (95% confidence level) in good agreement with Ruiz Etcheverry et al. (2016). In the northern region, the positive linear trends are associated with local changes in the density field caused by advective effects in response to a southward displacement of the South Atlantic High (Ruiz Etcheverry et al. 2016).

The continental shelf circulation is also affected by important interannual variability that mostly has its origin in the variability of the wind. In continental shelves, the alongshore component of both wind and ocean currents is the dominant one (Gill 1982). Using in situ and satellite altimetry as well as the time series of the SSH obtained from the tide gauge at Mar del Plata, Lago et al. (2021) showed that the alongshore component of the interannual variability of the transport in the northern portion of the shelf (at about 38°S) is significantly correlated with the Southern Annular Mode (SAM). This happens thanks to the geostrophic adjustment that occurs when the wind is parallel to the coast (Gill 1982). The same conclusion, i.e., that SAM explains a large portion of the interannual variability of the currents in the Patagonian shelf, was obtained using regional numerical models in the southern portion of the shelf by Combes and Matano (2018) and Guihou et al. (2020) and, using a global reanalysis model, by Bodnariuk et al. (2021a, b).

Findings reported here are in agreement with the increase in water temperature and sea level reported in the framework of the latest Intergovernmental Panel on Climate Change (IPCC) report for the southwestern Atlantic (Bindoff et al. 2013). The statistical confidence is quantified as low, moderate, or high in the IPCC report. The water temperature increase and sea level have a moderate confidence in the region (Bindoff et al. 2013). A decrease in dissolved oxygen concentration (low confidence) and in pH, increasing ocean acidification (high confidence), are also

predicted (Bindoff et al. 2013). In the Southern Hemisphere, the SAM influences the zonal asymmetry in the westerly winds and generates convergent and divergent transport in the Antarctic Circumpolar Current. In turn, the wind-driven currents in the Antarctic Circumpolar Current contribute to the regional asymmetry of decadal sea level variations during most of the twentieth century (IPCC 2014; Thompson and Mitchum 2014). Net regional sea level changes were estimated by the IPCC (2014) from a combination of the various contributions to sea level change (dynamic sea level, atmospheric loading, glacier mass changes, and ice sheet surface mass balance) derived from CMIP5 climate model outputs either directly or through downscaling techniques (Perrette et al. 2013; Kopp et al. 2014; Slangen et al. 2014; Bilbao et al. 2015; Carson et al. 2016). The contributions from groundwater depletion, reservoir storage, and dynamic ice sheet mass changes were not simulated by coupled climate models over the twentieth century and were estimated from observations. The sum of all contributions, including the glacio-isostatic adjustment contribution, provided a modelled estimate of the twentieth century net regional sea level changes that shows, for the Patagonian region, an increase that ranges between 100 and 200 mm in relative sea level (IPCC 2014).

Inner Shelf

Buenos Aires Coastal Waters

Baseline

The coastline of the Buenos Aires province is very extensive: it goes from the Rasa point (36.3°S), the exterior southern limit of the Río de la Plata estuary, to the mouth of the Negro river (41°S). The coastline can be divided in a northern and southern section, being Bahía Blanca (Fig. 3) the division point. In the northern section, there are a large number of beaches that are used for tourist and recreational purposes during the summer season and a series of cliffs that are being affected by erosion. The ports of Quequén and Mar del Plata are also in the northern region, the latter with serious sediment deposition problems. The southern section is known as El Rincón area and includes the Anegada bay (Fig. 3). El Rincón area is of great importance for the Patagonian Sea due to the exchange of water masses that occur in it and with the surrounding coastal areas. Inlets, marshes, tidal flats, and different types of beaches can be identified throughout the El Rincón region that is also strongly influenced by the continental discharge of the Colorado and Negro rivers. South of Anegada bay, the coast presents sandy beaches with little slope. The whole region is socially and economically important (see Narvarte et al. this volume). El Rincón area is a rich region for fishery production (Rodrigues et al. 2013; Jaureguizar et al. 2016), and the estuary of Bahía Blanca contains one of the most important industrial ports in Argentina. In both areas very large wetlands rich in flora and fauna must be protected and conserved to preserve the natural ecosystem that sustains fisheries and

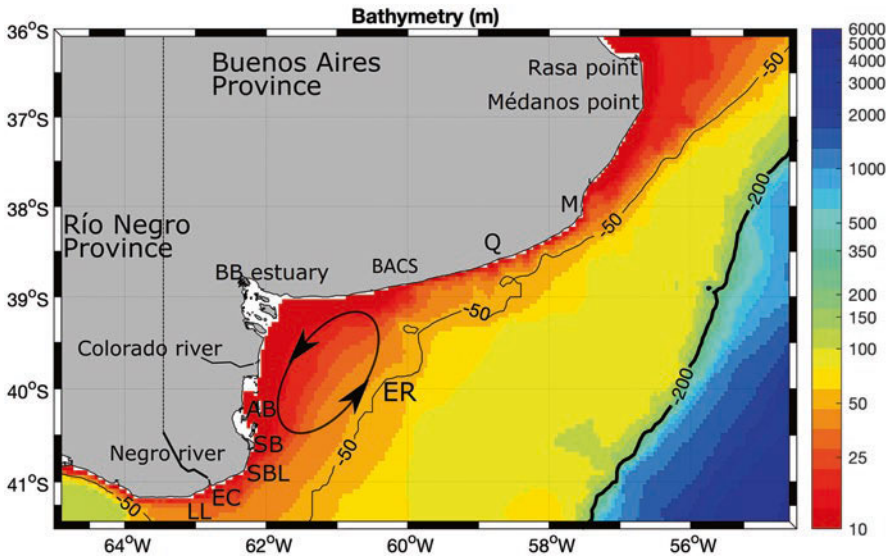

Fig. 3 Bathymetry (GEBCO 2020) for the Buenos Aires coastal waters; black thick and thin lines are the 200 and 50 m isobaths; geographical locations indicated are *BACS* Buenos Aires coastal shore, *M* Mar del Plata, *Q* Quequén, *BB* Bahía Blanca, *ER* El Rincón, *AB* Anegada bay, *SB* San Blas bay, *SBL* Segunda Barranca lighthouse, *EC* El Cóndor, and *LL* La Lobería (Bermeja point)

recreational activities and provides intangible well-being to the society. Yet, large changes, both of anthropogenic and natural origins, are registered in the region.

The circulation in the region is dominated by the alongshore component of the wind and by the tides (Palma et al. 2004; Lago et al. 2019, 2021). The largest changes in ocean circulation in this region are associated with atmospheric circulation which is dominated by the presence of the semipermanent South Atlantic anticyclone, centered approximately at 30°S. The tidal regime is predominantly semidiurnal, and the mean range increases along the coast, from 1.7 m at San Blas bay to 3 m at El Cóndor (SHN 2018).

One of the physical phenomena that most affects the coasts are waves. Wörner et al. (2019) reported that at the south of Bahía Blanca estuary, the waves that propagate from the southwest, west, northwest, north, and from the northeast are significantly more frequent than the waves coming from the south and southeast. The mean wave heights increase southward, from 0.72 m at Anegada bay to 1.26 m at Segunda Barranca lighthouse, and decrease south westward, reaching 0.48 m in front of La Lobería (Bermeja point). This would provide a higher percentage of southward and south-westward longshore currents.

The waters in the El Rincón area can be divided in two: (i) the coastal ones influenced by the river discharge and (ii) the waters influenced by the advection of shelf waters coming from the south and from the SMG (Guerrero 1998; Lucas et al. 2005). The estuarine system is formed by the Negro and Colorado rivers that discharge, on average, 950 m^3s^{-1} and 150 m^3s^{-1}, respectively, (BDHI 2020; COIRCO

2020) and have a seasonal variability (Lucas et al. 2005). The El Rincón estuarine system varies its area between 10,000 km^2 during the austral autumn-winter period and about 15,000 km^2 during austral spring-summer (Lucas et al. 2005). Lucas et al. (2005) indicate that the river discharge produces a low-salinity area strongly affected by the water masses that come from the SMG with high salinity, which generates a strong salinity gradient with low values near the coast. The surface fields show a maximum salinity gradient following the 40–50 m isobath (Lucas et al. 2005). The circulation of the El Rincón water masses presents an anticyclonic gyre during spring and summer and is more constrained to inshore areas during winter.

Reiter et al. (2019) explored the seasonal variability of temperature and salinity in the El Rincón area. During the austral winter, temperatures near the surface range from 8 to 10 °C in the coastal region and between 6 and 8 °C in the middle shelf. Near the bottom, winter waters along the coast are warmer (12 °C), while surface and bottom temperatures are similar (6 to 8 °C) in the middle shelf, indicating the importance of the vertical mixing process there. Winter salinity field shows minimum values (lower than 33) near the coast due to the larger discharge of freshwaters from the Negro and Colorado rivers. Winter salinity maps show a marked gradient toward the East, up to the 40–50 m isobath, where salinity is 34 due to the influence of the SMG water plume (Guerrero et al. 1997; Lucas et al. 2005). Further east, winter salinity decreases to 33.5. In spring, surface temperature increases up to 16 °C near the coast; river discharge is maximum, affecting the salinity field near the coast; and the salty waters from the SMG spread along the coastal strip up to the 40–50 m isobath. During summer, temperature in the El Rincón area is distributed homogeneously in the vertical, with large values (20 °C) from the coast up to the 50 m isobath, where a well-marked gradient is observed. The influence of the SMG high-salinity (34) waters is also observed in summer. Finally, in autumn, temperature decreases to 14–16 °C near the coast, the SMG water plume is clearly visible (with larger temperatures), and the vertical homogeneity and the horizontal gradient observed in summer remain. Salinity reaches the maximum values in the Bahía Blanca estuary region (up to 35) and minima (32) in the Anegada bay.

Observed Changes

Satellite altimetry results for the 1997–2017 period (Fig. 2c) suggest that the SSH trend goes from 3 mm yr^{-1} in El Rincón region up to 4.5 mm yr^{-1} in Bahía Blanca estuary, and between 3 and 4 mm yr^{-1} to the north of that site. The IPCC (2014) determined that the interaction of sea-level rise and changes in precipitation will have a more severe impact on shallow estuaries (<10 m) than on deep basin estuaries (>10 m) (Hallett et al. 2018; Elliott et al. 2019).

The IPCC Fifth Assessment Report confirms that the ocean is getting progressively warmer, with parallel changes in ocean chemistry such as in acidification and oxygen loss (Rhein et al. 2013). In the northern Patagonian region, the increase of the SST can be confirmed by the MODIS observations (Fig. 2a) with a positive trend of 0.2 °C decade^{-1} for the coastal region of El Rincón (up to 40–50 m isobath)

and a positive trend of 0.4 °C decade^{-1} toward the east. On the other hand, bottom temperatures do not show a significant trend at El Rincón for the period 1980–2016 (Elisio et al. 2020). Temperatures at El Rincón also show an irregular oscillation with periodicities between 3 and 7 years that could be in part due to the biennial and intra-decadal periodicities related to the high (2–4 years) and low (5–7 years) frequency components of the El Niño-southern oscillation variability (Guerrero 1998; Penland et al. 2013; Reiter et al. 2019; Elisio et al. 2020).

Finally, Pérez et al. (2017) found significant positive trends in wind waves near Mar del Plata, reaching maximum values of 16 mm per decade. Trends in the significant wave height were statistically different from zero only for the east and northeast directions. Negative trends (significantly different from zero, with 95% confidence) were obtained for waves coming from the southwest (Pérez et al. 2017). Echevarría et al. (2019) observed that the alongshore wave energy flux from Bahía Blanca estuary to Mar del Plata is related to the natural erosive and constructive processes detected.

North Patagonian Gulfs

Baseline

This section analyses the circulation of the North Patagonian gulfs, a region of the Argentinean Sea that is located between 40 and 43°S and includes the SMG, Nuevo gulf (NG), San José gulf (SJOG), and the Valdés peninsula (Fig. 4). The region constitutes one of the most important marine ecosystems in the Argentine Sea. Both the reservoir of coastal flora and fauna and the fishing resources (commercial and artisanal) have captured the attention and financial support of international organizations linked to the conservation and care of the environment. Also, the region has long been recognized for the high productivity and biodiversity of the ecosystem (Acha et al. 2004).

As in the rest of the continental shelf, in situ observations are scarce. In particular, current records are few and of short duration (Framiñan et al. 1991; Rivas 1997; Moreira et al. 2009; Saraceno et al. 2020) and mostly show that the region is dominated by high-frequency, inertial fluctuations and tides. The shortness of the time series is inadequate to reveal the mean circulation. For this reason, the average circulation in the area is mainly inferred from hydrographic data, biological indicators, and numerical models.

The geometry of the mouths of the three gulfs hampers the renewal of the waters inside of them. Therefore, waters within the gulfs are largely influenced by the local atmospheric forcing (Rivas 1990). While the surface heat flux changes direction throughout the year, the freshwater flow is always toward the atmosphere, since evaporation exceeds precipitation (Scasso and Piola 1988). These characteristics of the atmospheric flow and the limited renewal of its waters produce a greater annual thermal amplitude and relative maxima of salinity within the gulfs (Lucas et al.

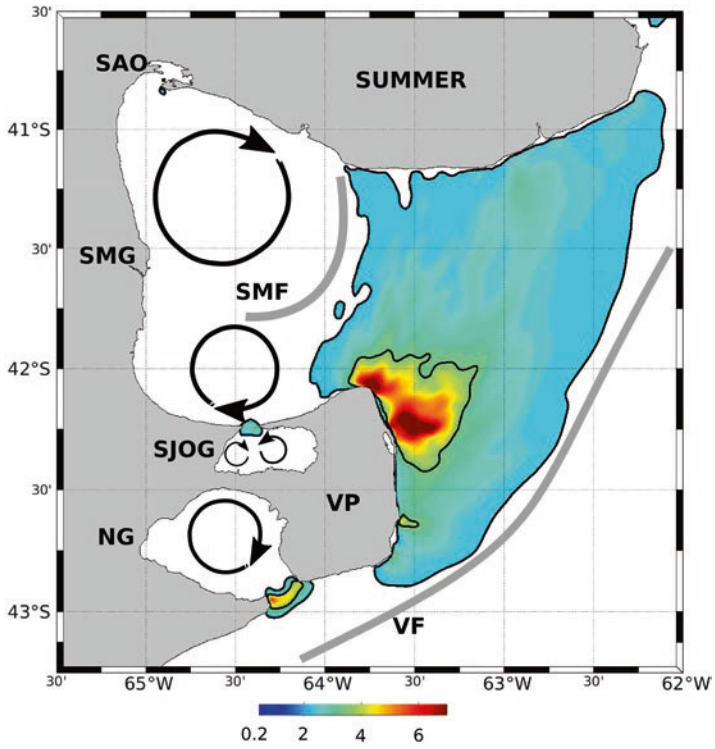

Fig. 4 Summer main features of North Patagonian gulfs. Background colors represent the tidal energy dissipation of the principal tidal constituent M2 [W m^{-2}]. The solid gray line indicates schematic locations of the thermal fronts (*SMF* San Matías front, and *VF* Valdés front), and the black solid line represents the main gyres into the gulfs. *SAO* San Antonio Oeste, *SMG* San Matías gulf, *SJOG* San José gulf, *NG* Nuevo gulf, and *VP* Valdés peninsula. (Adapted from Tonini and Palma 2017)

2005; Tonini et al. 2013). As noted in the previous section, the drainage of the relatively saline waters of the SMG through the north of the mouth invades the El Rincón estuary sector during winter (Lucas et al. 2005; Tonini et al. 2013). The main entrance of colder and less saline waters is through the southern sector of the mouth of the SMG (Rivas and Beier 1990).

The whole region is characterized by intense westerly winds and significant surface heat and freshwater fluxes (Scasso and Piola 1988), as well as a great amplitude of tides (Palma et al. 2004). Tides reach more than 9 m of maximum amplitude range inside SMG, at San Antonio Oeste (Fig. 4), 8 m in SJOG, 6 m in the NG, and over the Punta Norte-Valdés peninsula (SHN 2018). The bottom topography and the complex coastline are such that there is a phase shift of nearly a half period on both sides of the 7-km-long isthmus that separates NG from SJOG. This peculiarity, together with the large amplitude of the tides, has promoted the interest for the generation of tidal energy (Palma 2002). The interaction of the large tidal currents with

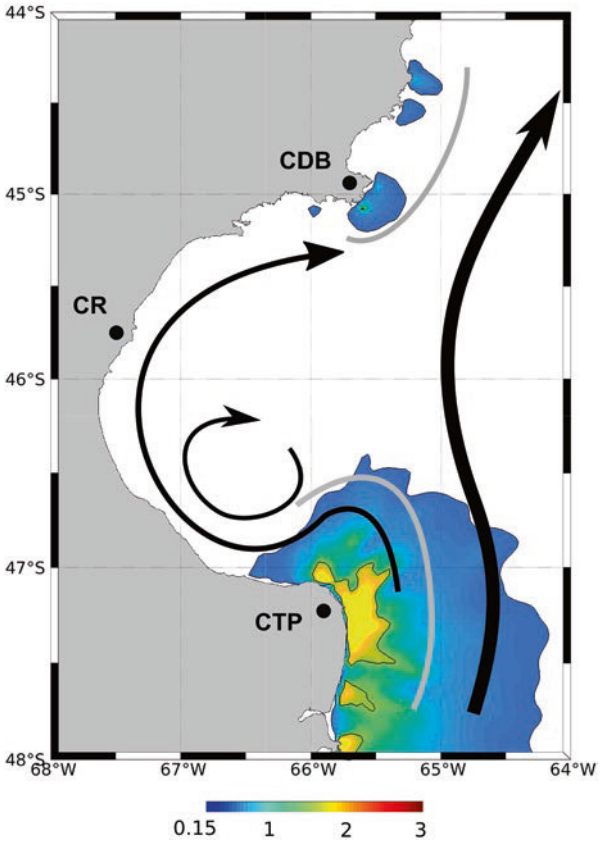

Fig. 5 Main features of San Jorge gulf. Background colors represent the tidal energy dissipation of the principal tidal constituent M2 [W m^{-2}]. The solid gray lines indicate schematic locations of the thermal fronts, and the black solid lines represent the main summer circulation. *CDB* Dos Bahías cape, *CR* Comodoro Rivadavia, and *CTP* Tres Puntas cape. (Adapted from Palma et al. 2020)

the complex irregular bottom topography produces in the region one of the highest energy dissipation rates of the South Atlantic ocean (Fig. 5; Palma et al. 2004). The latest numerical simulations in the region (Tonini and Palma 2017) improved its accuracy, thanks to several in situ measurements: a 22-month time series of bottom pressure measurements that was obtained close to the northern coast of the SMG (Lago et al. 2017) and other four coastal stations where current-meter measurements were obtained (Moreira et al. 2011). The authors showed that the total area-integrated energy tidal dissipation attains 27.9 GW. This result is larger than the one calculated by Moreira et al. (2011) and is in close correspondence with the 28 GW computed by Palma et al. (2004). The value represents ~24% of the total energy dissipated in the Southwestern Atlantic shelf (Palma et al. 2004). The vertical

mixing induced by the tidal energy in combination with the increased heat fluxes in spring and summer allows the homogenization of the water column in shallow areas and the occurrence of thermal fronts that separate these well-mixed waters from the stratified waters. Indeed, one of the most important frontal zones of the Argentine shelf is the Valdés front (VF, Fig. 4), located near Valdés peninsula in a SW-NE direction (Fig. 4) (Glorioso 1987; Romero et al. 2006). Also, near the mouth of the SMG, a thermal front (SMF, Fig. 4) delimits the internal circulation of the gulf from external waters (Gagliardini and Rivas 2004; Tonini et al. 2013; Pisoni et al. 2015). Associated with the dynamics of these frontal systems, there is a high rate of primary and secondary productivities that constitute key ocean structures to understand the feeding, reproduction, and migratory patterns of local populations of birds and mammals, as well as important fishing resources (Sabatini and Martos 2002; Acha et al. 2004).

The latest advances in the dynamical knowledge of the region were provided from numerical simulations (Tonini et al. 2013; Tonini and Palma 2017). One of the main results is that tidal forcing, stratification, and winds significantly contribute to the overall subtidal residual circulation of the region. The model shows that the nonlinear interaction between the oscillating tide and bottom topography leads to the formation of several robust residual circulation patterns, basin gyres, bathymetric vortices, and coastline quadrupoles, which are formed by recirculating eddies at the mouths of SJOG and NG. The results of the numerical simulations also show inside SMG that the overall summer circulation pattern is dominated by a strong cyclonic gyre (composed by two recirculating sub-gyres) (Fig. 4). As a result of this closed circulation, the gulf is almost isolated from the shelf during summer. The location and direction of circulation of the gyres of the SMG were advanced by means of an analysis of hydrographic data by Piola and Scasso (1988) and partially confirmed by direct measurements in a station near the north gyre by Framiñan et al. (1991). Although the velocities provided by the numerical model (ROMS, Tonini et al. 2013) show the correct temporal direction and intensification, they are somewhat lower than the measurements (~15 cm s^{-1} on average) and require a greater number of long-term direct measurements (currents) to allow calibration and validate the results. The summer circulation pattern was validated for the first time by the trajectory of five drifters deployed in the northern sector of the SMG (Saraceno et al. 2020). The drifters also showed the presence of small-scale features that are not observed with the climatological forced models. In particular, a strong filament that detaches from the western coast and advects coastal waters to the middle of the gulf was observed with both the drifters and high-resolution satellite color images (Saraceno et al. 2020). Within the coastal jet, nontidal currents can be as large as 21 cm s^{-1}. Similar velocities have been observed closer to the coast with current-meter measurements (Moreira et al. 2009).

The numerical model results of the same authors also show that in winter, when the stratification is eroded and the northern sub-gyre spins down and gradually shrinks in size, the western sector of the gulf is occupied by an anticyclonic gyre. The wind forcing strengthens both the cyclonic and anticyclonic circulation during fall-winter.

In the NG the dynamics is similar to the one observed in the SMG. However, in the NG there is only 1 year-round cyclonic gyre (Fig. 4) that intensifies in summer and is reduced in spatial extension in winter, with the appearance of a weak anticyclonic gyre in the western coast. The cyclonic gyre of NG was observed remotely from optical and thermal channels of the Landsat-TM (Gagliardini 2011), and in both gulfs (NG and SMG), vertical profiles show a dome shape of the isopycnals in the center of the gulfs, indicative of a cyclonic circulation (Pisoni 2012; Tonini et al. 2013).

The SJOG (Fig. 4) has a very different seasonal behavior. In summer, it can be separated in two domains with different dynamics and thermal characteristics: the western domain is more affected by strong tidal currents than the eastern domain. As a consequence, waters are warmer on the surface, and vertical stratification is set up in the eastern domain during summer. In winter, the entire gulf is vertically homogeneous (Esteves et al. 1986). Using satellite remote sensing data, Amoroso and Gagliardini (2010) observed vortices and jets in the western domain of the SJOG and in the south of the SMG. These patterns are generated by the exchange of waters between the SJOG and SMG and are clearly visible also in high-resolution numerical simulations (Tonini and Palma 2017).

Observed Changes

Satellite altimetry measurements show a trend of the SSH of up to 4.6 mm yr^{-1} in the northwest coast of SMG and of about 3 mm yr^{-1} in NG (Fig. 2; Ruiz Etcheverry et al. 2016). Values at San Antonio Oeste are among the largest in the entire Argentine shelf. Yet, given the large tidal amplitude in this region (see above) and the vicinity of the coast that affects satellite altimetry measurements, results should be interpreted with care.

Given the southward migration of the semipermanent South Atlantic high-pressure system (Barros et al. 2008; Blázquez et al. 2012), a higher frequency of northerly winds can be expected over this region of the Patagonian coast. This scenario could favor the occurrence of coastal upwelling events described in Pisoni et al. (2014). On the other hand, a decrease in the mixed-layer depth (5 m per decade) was estimated by a global numerical model in the SMG and NG according to Franco et al. (2018) between 2003 and 2017. This change should have strongly affected the summer circulation, the transport of the main gyres, and the local ecosystem. Yet, evidence of such changes based on observations have not been reported so far.

Despite the absence of published works related to the climatic effects on the circulation and dynamics of the north Patagonian gulfs, numerical models could be one of the keys to explore possible future scenarios at low cost based on the trending physical variables shown by satellite or studies in other regions of the world. The region of the north Patagonian gulfs remains largely an unexplored region, especially in terms of in situ observations. The studies carried out lack precision due to the scarce direct measurement of physical variables. With the help of tools such as

numerical models and satellite images, large spatial and temporal gaps are covered that help to understand the dynamics of the region and thus predict future changes.

San Jorge Gulf

Baseline

San Jorge gulf (SJG) constitutes a complex ecosystem that provides a variety of important services to the regional economy, as oil (Sylwan 2001), fisheries (Glembocki et al. 2015; Temperoni et al. 2018), and tourism (St-Onge and Ferreyra 2018). At the same time, the gulf constitutes one of the regions with the greatest biodiversity of the Patagonian shelf (see chapters by Galván et al. this volume and Crespo this volume).

The SJG is the largest gulf of the Patagonian coast of Argentina. With an extension of nearly 40,000 km^2, it is located between Dos Bahías and Tres Puntas capes (Fig. 5). The center of the basin is deeper than 100 m. The gulf mouth extends for approximately 250 km, with shallower depths at the southern end (Fig. 5).

There are no rivers that flow into the gulf, and evaporation exceeds precipitation in the whole area (ECMWF ERA-40 Atlas, https://sites.ecmwf.int/era/40-atlas/docs/section_B/parameter_emp.html). The Patagonian region is influenced by mid-latitude westerlies, which are strongest in the latitude of this gulf (Labraga 1994). Tides are semidiurnal, with a mean amplitude of 4.18 m in Comodoro Rivadavia (the main city on the gulf coast, Fig. 5) and a maximum of 6.09 m (SHN 2018). The bottom friction produced by the interaction of the tidal currents and shallow banks located near Tres Puntas cape produces one of the largest tidal dissipation areas of the Patagonian shelf (Palma et al. 2004; Moreira et al. 2011).

SJG waters are a mixture of waters of subantarctic origin, modified by air-sea heat fluxes and low-salinity waters from the South, advected by the Patagonian current (Brandhorst et al. 1971; Palma and Matano 2012). During summer, the pycnocline reaches 40–50 m depths, deepening to exceed 60 m in autumn (Cucchi-Colleoni and Carreto 2001). Intrusions of low-salinity waters from the Patagonia current at intermediate depths have been reported in autumn (Krock et al. 2015) and summer (Carbajal et al. 2018).

The vertical structure is homogeneous in winter and stratified during summer in much of the gulf (Torres et al. 2018). The summer pycnocline, approximately matching the depth of the euphotic zone, separates surface nutrient-poor, oxygen-rich waters from deeper nutrient-rich, oxygen-poor waters (Torres et al. 2018). In the north and south of the gulf mouth, the water column remains vertically homogeneous even in summer due to tidal mixing with high dissipation rates (Fig. 5; Palma et al. 2004), favoring the generation of tidal fronts (Acha et al. 2004; Rivas and Pisoni 2010; Glembocki et al. 2015; Carbajal et al. 2018; Flores-Melo et al. 2018). Carbajal et al. (2018) have found variations in the position of the tidal front of approximately 8 km near spring tide and 4 km prior to neap tide, although baroclinic instabilities can significantly modify the shape and position of the front (Carbajal

et al. 2018; Flores-Melo et al. 2018). Furthermore, the authors have found great variability in Chl *a* concentrations between both tidal phases, suggesting a greater intrusion of subsurface waters during neap tide.

As current velocity data are scarce within the SJG, up-to-date knowledge on gulf dynamics is based mainly on the outputs of numerical simulations. Recently, Matano and Palma (2018) and Palma et al. (2020) described the seasonal circulation in SJG. During summer, an inner portion of the Patagonian current enters the SJG, generating a loop that merges with an intense cyclonic coastal current (Fig. 5). The loop and the coastal current enclose a recirculating cyclonic gyre in the southern basin. In the northern sector, a weak and elongated anticyclonic coastal gyre is developed, while the interior circulation is composed of a slow anticyclonic gyre bounded in the west by the coastal current and by a broad northward flowing current in the east. These two currents encounter before exiting the SJG as an intense jet through its northern edge (Dos Bahías cape). From late fall to early winter, the Patagonian current moves offshore, thus reducing its penetration into the gulf. During winter, the cyclonic coastal current and the southern gyre weaken, and anticyclonic patterns are developed in the southern region. Furthermore, the southeast anticyclonic gyre expands, blocking a large portion of the mouth, thus shifting the inflow of Patagonian shelf waters to the north. Increasing stratification during spring leads to an intensification and expansion of the cyclonic circulation, and, by the end of December, the summer circulation pattern is fully developed. Superimposed on these seasonal circulation patterns, there is an anticyclonic gyre over the southern bank that persists year-round. The largest exchange with the shelf occurs in summer, mainly at the surface and at intermediate layers and confined to the northern region. Then, waters are replaced with waters mostly coming from the Patagonian current (Palma et al. 2020).

There are very few measurements of currents in the gulf. Mean velocities from three drifting buoys deployed near Comodoro Rivadavia city ranged between 0.27 and 0.38 m s^{-1}, with maxima of ±1.50 m.s^{-1} inside the SJG (Esteves et al. 2012). During November 2017, reversal velocities near 0.4 m s^{-1} associated to tidal currents were registered in the northern region close to the mouth, with maxima that exceeded 1 m s^{-1} (Pisoni et al. 2020). In March 2020, maximum velocities of approximately 0.5 m s^{-1} were detected in a shallow region (< 30 m) in the north of SJG.

Observed Changes

As well as tidal mixing, coastal upwelling is also a mechanism that favors the ascent of nutrients from deeper layers. Although westerly winds on the east coast of Patagonia are not favorable to upwelling (Matano et al. 2010), given the semicircular shape of the SJG, favorable conditions can be generated on the southern coast of the gulf (Tonini et al. 2006; Pisoni et al. 2020). It is expected that an increase in the intensity of the westerlies (Thompson et al. 2011) will have an impact on the coastal

upwelling (see however Pessacg et al. this volume). In addition, another mechanism for input of nutrients into the sea is due to the contribution of dust transported by the atmosphere. In the Patagonian shelf, dust contribution to primary productivity is a subject of active research: Johnson et al. (2011) concluded that atmospheric fluxes of mineral dust from Patagonia are not likely to be the major source of bioavailable iron to ocean regions characterized by high primary productivity; similarly, a recent study that combined a long record of in situ terrestrial dust, satellite data of Chl *a* and currents suggested that dust from Tierra del Fuego is not a source of nutrients for the Chl *a* blooms observed (Cosentino et al. 2020). On the other hand, Paparazzo et al. (2018) observed a bloom after a dust event in the NG coastal area. In a context of intensification of the westerly winds, dust storms could favor the fertilization of the ocean if its role as a fertilizer is confirmed in the area.

A positive trend in SST of about 0.3 °C per decade is shown in Fig. 2a. Recently, Leyba et al. (2019) found a significant positive trend in SST during winter over much of SJG, not being significant in summer. On the other hand, the sea level anomaly trend found within SJG is one of the smallest ones along the Patagonian coast (Fig. 2c; Ruiz Etcheverry et al. 2016).

Finally, Marrari et al. (2016) found an increase of 2% per year of Chl *a* concentration within the SJG since 1997. This positive trend is mainly located in the coastal regions (depth < 50 m) west and south of the GSJ (Fig. 2b; Marrari et al. 2016).

The Southern Patagonia Shelf, Beagle Channel, and Magellan Strait

Baseline

The properties and dynamics of the water masses present in the southern Patagonian shelf (SPS) and associated channels and straits south of 47°S are largely influenced by the inflow of diluted subantarctic waters coming from the Pacific ocean. This connection is provided by the eastward outflow of the Magellan strait (Brun et al. 2020) and the Cape Horn current (Strub et al. 2019), a branch of the West Wind Drift that flows poleward along the Pacific coast of South America from 40°S. Upon encountering Cape Horn, the waters transported by the Cape Horn current are advected northeastward by another branch of the Antarctic Circumpolar current and enter the SPS through the Le Maire strait and the passage east of Isla de los Estados (Guihou et al. 2020; see Fig. 6 for geographical locations).

The precipitation regime in the Magallanes-Tierra del Fuego region exhibits a distinct longitudinal gradient, with a sharp discontinuity marked by the Andes mountain range. Humidity from the Pacific ocean is pushed by the prevailing westerlies, which produces high precipitation rates by orographic control on the western side of the Andes. On the contrary, dry winds and relatively low precipitations are a common feature east of the cordillera. Together with direct rainfall, seasonal (spring-summer) inputs from snow and ice melting also contribute to freshwater

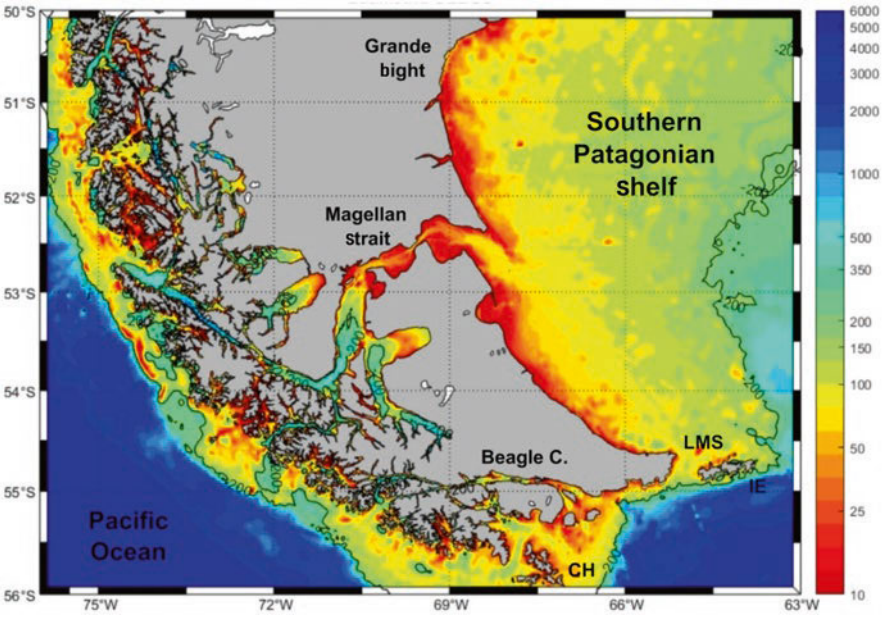

Fig. 6 Bathymetric chart (depth in meters) of the southern Patagonian shelf. CH, LMS, and IE correspond to Cape Horn, Le Maire strait, and Isla de los Estados, respectively

inputs. The precipitation/runoff excess on the Pacific side results in a significant dilution of subantarctic waters in the southeastern Pacific, a signal that, helped by the regional circulation, propagates to the Patagonian shelf and can be traced as far north as SJG (Acha et al. 2004) or even the SMG according to Palma and Matano (2012). The northeastward flow of waters of Pacific origin has been estimated as 0.88 Sv at 51°S by Guihou et al. (2020).

The west coast of the Andes presents a complex morphology inherited from the combined action of tectonic movements and successive glaciations during the Quaternary (Rabassa and Clapperton 1990; Rabassa 2008; see Isla and Isla this volume). These cycles have carved a vast network of fjords, channels, and archipelagos extending from 42°S to Cape Horn (56°S). Some of these erosive marks, namely, the Magellan strait and the Beagle channel, have evolved into uninterrupted conduits that put in contact the Pacific and Atlantic oceans and thus must be considered together with the inflow across Cape Horn in the total transport of water and – mainly – properties into the Atlantic Patagonian shelf.

In its equatorward transit, the flow of waters of Pacific origin is supposed to also entrain part of the Beagle channel outflow before entering the SPS. Further north, the plume of relatively freshened waters is further diluted upon encountering the mouth of the Magellan strait at 52°S. Even though the flow through the Le Maire strait and the shelf-break dominates the volume transport into the SPS (Guihou et al. 2020), the outflow of the Magellan strait at 52°S is considered as the most significant contributor to the freshening of the SPS waters (e.g., Palma and Matano 2012).

The circulation in the SPS is complex due to its abrupt bathymetry, but the net transport is directed to the north and northeast, as a tongue of freshened waters mixed by winds and tides (Palma et al. 2008; Palma and Matano 2012). This body of freshened water, called the Magellan plume, progresses northward along the SPS controlled by the combined effects of the wind, tides, and western boundary currents (Palma et al. 2004; Palma and Matano 2012). Around the Magellan strait, the combination of strong tidal mixing and low-salinity coastal plumes generates frontal systems which show a semi-annual cycle changing their orientation from summer to winter (Rivas and Pisoni 2010).

The dominant winds interact with the morphology of the Grande bight at 52°S, resulting in a counterclockwise gyre at its southern part (Glorioso and Flather 1995; Palma et al. 2008). Cool and freshened northward flowing waters that originate in the Cape Horn current and the Magellan strait encounter that anticyclonic gyre of warm waters, forming a conspicuous front that extends northeastward from Grande bight. Flow divergence results in upwelling motions that may sustain the high primary and secondary biological production observed in the Grande bight and its surroundings (Schloss et al. 2007; Sabatini et al. 2016).

The Magellan Strait

The strait stretches for almost 600 km along a tortuous path, starting in the Pacific coast and opening to the Patagonian shelf at 52.5°S. The width and depth of the strait vary dramatically along its course, with depths >1,000 m at the Pacific entrance and only 70 m at the Atlantic mouth. Tidal amplitudes are also contrasting, from 1.2 m in the west to more than 7 m at its eastern limit (Panella et al. 1991; Fierro 2008). The net flow is, like in the rest of the region, eastward (e.g., Panella et al. 1991), implying a transfer to the Patagonian shelf of the freshened waters that infill the Magellan strait. Subantarctic waters enter the strait from the west and are progressively modified by continental inputs. At the Atlantic exit, modified subantarctic waters (Sievers and Silva 2008) with salinities 31–32 are injected into the SPS. Recently, Brun et al. (2020) estimated a net transport from the Pacific to the Atlantic along the Magellan strait of the order of 50,000 $m^3\ s^{-1}$.

The Beagle Channel

Together with the interoceanic gateway that the Magellan strait represents, another uninterrupted though tortuous passage at latitude 55°S connects the Pacific ocean with the eastern coasts of South America: the Beagle channel. This 300-km-long conduit displays a very variable bathymetry, comprising small basins and bays with depths up to 400 m intervened by narrow and shallow sills 10–20 m deep. These features, combined with important freshwater inputs, have led some authors to suggest that the channel displays a fjord-like circulation (Isla et al. 1999). The mean

surface flow is eastward, that is, from the Pacific to the Atlantic ocean (Balestrini et al. 1998), while more complex flow patterns are observed inside bays (Flores-Melo et al. 2020). In areas deeper than 50 m, the Beagle channel displays a seasonal cycle of vertical stratification, mainly controlled by freshwater inputs during spring and summer. In winter, reduced runoff and air-sea heat losses trigger the complete mixing of the water column by convection (Flores-Melo et al. 2020). The combination of seasonal stratification, sluggish flow, relatively high residence times (Cucco et al. 2019), and relevant inputs of organic matter from both natural and anthropogenic sources (Gil et al. 2011) result in the depletion of oxygen concentrations near the bottom at some sectors of the channel. This condition is particularly notable near the city of Ushuaia (Martin et al. 2016; Flores-Melo et al. 2020).

Tides in the channel are meso-microtidal with a range of amplitudes 0.67–2.18 m (D'Onofrio et al. 2016), contrasting with amplitudes up to 10 m in the northern sector of the SPS.

Observed Changes and Possible Consequences

Projections by IPCC (2014) signal high-latitude environments as those to be more likely affected by large climatic changes in the near future. The transport at the southernmost tip of South America is governed by a net transfer of water from the coastal Pacific to the Atlantic Patagonian shelf. Such transport is mediated by the prevailing westerlies and buoyancy forces. South of 50°S, winds impinging on the Pacific coast and associated precipitations have been increasing during the last decades according to Garreaud et al. (2013). Such changes can be associated with the observed positive trend of the SAM, which in turn has been associated with anthropogenic forcing (Marshall et al. 2006). The positive SAM trend reported by Marshall et al. (2006) would also lead to significant changes in the water mass characteristics (lower salinity) of the SPS (Guihou et al. 2020).

In fact, glacier retreat is being observed in the large ice fields of southern Patagonia (Bown et al. 2019) and is well documented in the eastern limit of the glacier distribution (Strelin and Iturraspe 2007).

An increase in freshwater inputs would result in an intensification of the Cape Horn current, implying larger water transports and increased dilution in the Patagonian shelf. In particular, in environments like the Beagle channel where tides are not strong enough to mix the water column, the strength of vertical stratification should increase in response to an eventual rise of runoff and water temperature, leading to a potential increase of frequency and intensity of hypoxic events.

Final Remarks

In this chapter we reviewed the main forcings that drive the ocean circulation in the Patagonian shelf with focus in the coastal regions. We also computed trends of satellite variables: SST, SSH, and Chl *a*. A significant positive trend (up to 0.04 °C per

year) north of ~50°S and negative values (up to −0.02 °C per year) south of 50°S are observed. The negative SST trend observed in the southern portion of the region is associated with the positive trend observed in the dominant westerly winds within those latitudes. The spring Chl *a* linear trend observed shows values as large as 2 mg m^{-3} over a 10-year period in the outer portion of the continental shelf between 50 and 40°S. The linear trend in SSH ranges between 2 and 5 mm yr^{-1} (95% confidence level) in good agreement with previous results. In the northern region, the positive linear trends are associated with local changes in the density field caused by advective effects in response to a southward displacement of the South Atlantic High. Recent studies show that the SAM is one of the main players that might explain a portion of the interannual variability observed in the Patagonian shelf. Findings reported here are in agreement with the main results and predictions reported in the IPCC report for the southwestern Atlantic (IPCC 2014). A decrease in dissolved oxygen concentration and in pH (increasing ocean acidification) are also predicted (Bindoff et al. 2013).

In the northern Patagonian gulfs, the southward migration of the semipermanent South Atlantic High pressure system will induce a higher frequency of northerly winds. This scenario could favor the occurrence of coastal upwelling events and a decrease in the mixed-layer depth of up to 5 m per decade, as estimated by a global numerical model in the SMG and NG between 2003 and 2017 (Franco et al. 2018).

In SJG, more favorable upwelling conditions can be generated on the southern coast of the gulf as the result of an increase in the intensity of the westerlies that is expected as part of the climate change for these latitudes (Thompson et al. 2011).

In the southern Patagonia shelf, the increase of winds in the Pacific coast and associated precipitation can be associated with the observed positive trend of the SAM and affect the net transfer of water from the coastal Pacific to the Atlantic Patagonian shelf and therefore significant changes in the water mass characteristics (lower salinity) of the southern Patagonia shelf.

Accurate long time series of multiple physicochemical parameters is the limiting factor to produce the necessary knowledge to be able to adapt to and mitigate the climate change that the region is facing. Such measurements are difficult and expensive to obtain. Yet, they can make the difference to have the chance to preserve the Patagonian Sea as a healthy and productive ecosystem.

References

Acha EM, Mianzan HW, Guerrero RA, Favero M, Bava J (2004) Marine fronts at the continental shelves of austral South America: physical and ecological processes. J Mar Syst 44:83–105

Amoroso RO, Gagliardini DA (2010) Inferring complex hydrographic processes using remote-sensed images: turbulent fluxes in the Patagonian gulfs and implications for scallop metapopulation dynamics. J Coast Res 26:320–332

Andreo VC, Dogliotti AI, Tauro CB (2016) Remote sensing of phytoplankton blooms in the continental shelf and shelf-break of Argentina: spatio-temporal changes and phenology. IEEE J Sel Top Appl Earth Obs Remote Sens 9:5315–5324

Barros VR, Doyle ME, Camilloni IA (2008) Precipitation trends in southeastern South America: relationship with ENSO phases and with low-level circulation. Theor Appl Climatol 93:19–33

Beron-Vera FJ, Bodnariuk N, Saraceno M, Olascoaga MJ, Simionato C (2020) Stability of the Malvinas current. Chaos 30:13152

Balestrini C, Manzella G, Lovrich GA, (1998) Simulación de corrientes en el Canal Beagle y Bahía Ushuaia, mediante un modelo bidimensional. Servicio de Hidrografía Naval 98:1–58

BDHI (2020) Base de Datos Hidrológica Integrada, Secretaría de Infraestructura y Política Hídrica de la Nación. http://bdhi.hidricosargentina.gob.ar/. Accessed 19 June 2020

Bilbao RAF, Gregory JM, Bouttes N (2015) Analysis of the regional pattern of sea level change due to ocean dynamics and density change for 1993–2099 in observations and CMIP5 AOGCMs. Clim Dyn 45:2647–2666

Bindoff NL, Stott PA, Achuta Rao KM, Allen MR, Gillett N, Gutzler D, Hansingo K, Hegerl G, Hu Y, Jain S, Mokhov II, Overland J, Perlwitz J, Sebbari R, Zhang X, (2013) Detection and Attribution of Climate Change: from Global to Regional. In: Stocker TF et al. (eds) Climate Change 2013: The Physical Science Basis. Contribution of Working Group I to the Fifth Assessment Report of the Intergovernmental Panel on Climate Change, Cambridge University Press, Cambridge, United Kingdom and New York, NY, USA, pp 867–952. https://doi.org/10.1017/CBO9781107415324.022

Blázquez J, Nestor Nuñez M, Kusunoki S (2012) Climate projections and uncertainties over South America from MRI/JMA Global Model Experiments. Atmos Clim Sci 02:381–400

Bodnariuk N, Simionato CG, Osman M, Saraceno M (2021a) The Río de la Plata plume dynamics over the southwestern Atlantic continental shelf and its link with the large scale atmospheric variability on interannual timescales. Cont Shelf Res 212(2):104296. https://doi.org/10.1016/j.csr.2020.104296

Bodnariuk N, Simionato CG, Saraceno M (2021b) SAM-driven variability of the southwestern Atlantic shelf sea circulation. Cont Shelf Res 212:104313. https://doi.org/10.1016/j.csr.2020.104296

Boyer TP, Antonov JI, Baranova OK, Coleman C, Garcia HE, Grodsky A, Johnson DR, Locarnini RA, Mishonov AV, O'Brien TD, Paver CR, Reagan JR, Seidov D, Smolyar IV, Zweng MM (2013) World Ocean Database. Sydney Levitus (Ed), Alexey Mishonov (Technical Ed), NOAA Atlas NESDIS 72, 209 pp. https://doi.org/10.7289/V5NZ85MT

Brandhorst W, Castello JP, Perez Habiaga R, Roa BH (1971) Argentina: Evaluación de los recursos de anchoita (*Engraulis anchoita*) frente a la Argentina y Uruguay. 4. Abundancia relativa entre las latitudes 34grad.30 y 44grad.10 en relación a las condiciones ambientales en Ago-Sep 1970. FAO

Brun AA, Ramirez N, Pizarro O, Piola AR (2020) The role of the Magellan strait on the southwest South Atlantic shelf. Estuar Coast Shelf Sci 237:106661

Bown F, Rivera A, Peętlicki M, Bravo C, Oberreuter J, Moffat C (2019) Recent ice dynamics and mass balance of Jorge Montt Glacier, Southern Patagonia Icefield. J Glaciol, 65:253:732–744

Carbajal JC, Luján Rivas A, Chavanne C (2018) High-frequency frontal displacements south of 6 Jorge gulf during a tidal cycle near spring and neap phases: biological implications between tidal states. Oceanography 31:60–69

Carranza MM, Gille ST, Piola AR, Charo M, Romero SI (2017) Wind modulation of upwelling at the shelf-break front off Patagonia: observational evidence. J Geophys Res Ocean 122:2401–2421

Carson M, Köhl A, Stammer DA, Slangen AB, Katsman CA, van de Wal RSW, Church J, White N (2016) Coastal sea level changes, observed and projected during the 20th and 21st century. Clim Chang 134:269–281

COIRCO (2020) Comité Interjurisdiccional del Río Colorado. https://www.coirco.gov.ar/. Accessed 19 Jun 2020.

Combes V, Matano RP (2018) The Patagonian shelf circulation: drivers and variability. Prog Oceanogr 167:24–43

Cosentino NJ, Ruiz-Etcheverry LA, Bia GL, Simonella LE, Coppo R, Torre G, Saraceno M, Tur VM, Gaiero DM (2020) Does satellite chlorophyll-a respond to southernmost Patagonian dust? A multi-year, event-based approach. J Geophys Res Biogeosci. https://doi.org/10.1029/2020JG006073

Crespo EA (this volume) Long-term population trends of Patagonian marine mammals and their ecosystem interactions in the context of climate change. In: Helbling EW, Narvarte MA, González RA, Villafañe VE (eds) Global change in Atlantic coastal Patagonian ecosystems. A journey through time. Springer, Cham

Cucchi-Colleoni D, Carreto JI, (2001) Variación estacional de la biomasa fitoplanctónica en el Golfo San Jorge. Resultados de las campañas de investigación OB-01/00. OB-03/00, OB-07/00, OB-10/00 y OB-12/00. Inf Téc Int DNI-INIDEP, 49:30.

Cucco A, Martín J, Quattrocchi G, Fernández D, (2019) Water Circulation in the Beagle Channel, a modeling study. Geophys Res Abs, Vol. 21, EGU2019-2617.

D'Onofrio EE, Oreiro FA, Grismeyer WH, Fiore MME (2016) Accurate astronomical tide predictions calculated from satellite altimetry and coastal observations for the area of Isla Grande de Tierra del Fuego, Isla de los Estados and Beagle channel. Geoacta (Argentina) 40:60–75

Echevarría ER, Dragani WC, Wörner S (2019) A comprehensive study about alongshore wave energy flux in the coast of Buenos Aires, Argentina. J Coast Conserv 23:435–443

Egbert GD, Bennett AF, Foreman MGG (1994) TOPEX/POSEIDON tides estimated using a global inverse model. J Geophys Res. https://doi.org/10.1029/94jc01894

Elliott M, Day JW, Ramachandran R, Wolanski E (2019) Chapter 1 – A Synthesis: What Is the Future for Coasts, Estuaries, Deltas and Other Transitional Habitats in 2050 and Beyond? In: Wolanski E et al (eds) Coasts and Estuaries. Elsevier, pp 1–28. ISBN: 9780128140031.

Elisio M, Maenza RA, Luz Clara M, Baldoni AG (2020) Modeling the bottom temperature variation patterns on a coastal marine ecosystem of the southwestern Atlantic Ocean (El Rincón), with special emphasis on thermal changes affecting fish populations. J Mar Syst 212:103445

Esteves JL, Solis M, Cejas J, Vera R, (1986) Golfo San José: Resultados de las campañas oceanográficas 1984/1985. Report. Chubut, Argentina: Chubut Province Administration, 13p.

Esteves JL, Rivas A, Pisoni JP, Ocariz H, Troisi A (2012) Uso de las boyas SVP para el análisis de la circulación superficial en el golfo San Jorge y zona de influencia. VIII Jornadas Nacionales de Ciencias del Mar 2012, Comodoro Rivadavia, Argentina.

Flores-Melo X, Schloss I, Chavanne C, Almandoz G, Latorre M, Ferreyra G (2018) Phytoplankton ecology during a spring-neap tidal cycle in the southern tidal front of San Jorge gulf, Patagonia. Oceanography 31:70–80

Framiñan MB, Balestrini CF, Bianchi A, Demilio G, Piola AR (1991) Datos CTD y series temporales de velocidad, temperatura y conductividad en el golfo San Matías. Servicio de Hidrografía Naval, Informe Técnico N° 63/1991, Argentina.

Franco BC, Palma ED, Combes V, Acha EM, Saraceno M (2018) Modeling the offshore export of Subantarctic shelf waters from the Patagonian shelf. J Geophys Res Ocean 123. https://doi.org/10.1029/2018JC013824

Fierro J (2008) Tides in the austral Chilean channels and fjords. Avances en el conocimiento oceanográfico de las aguas interiores chilenas, Puerto Montt a cabo de Hornos. Silva N, Palma S, (eds). Comité Oceanográfico Nacional, Pontificia Universidad Católica de 669 Valparaíso, Valparaíso, pp. 63–66.

Gagliardini DA, Rivas AL (2004) Environmental characteristics of San Matías gulf obtained from LANDSAT-TM and ETM+ data. Gayana 68:186–193

Gagliardini DA, (2011) Medium Resolution Microwave, Thermal and Optical Satellite Sensors: Characterizing Coastal Environments Through the Observation of Dynamical Processes. In Remote Sensing of the Changing Oceans pp. 251–277. Springer, Berlin, Heidelberg.

Galván DE, Bovcon ND, Cochia PD, González RA, Lattuca ME, Ocampo Reinaldo M, Rincón-Díaz MP, Romero MA, Vanella FA, Venerus LA, Svendsen GM (this volume) Changes in the

specific and biogeographic composition of coastal fish assemblages in Patagonia, driven by climate change, fishing, and invasion by alien species. In: Helbling EW, Narvarte MA, González RA, Villafañe VE (eds) Global change in Atlantic coastal Patagonian ecosystems. A journey through time. Springer, Cham

Garreaud R, Lopez P, Minvielle M, Rojas M (2013) Large-scale control on the Patagonian climate. J Clim 26:215–230

GEBCO Compilation Group (2020) GEBCO 2020 Grid, https://doi.org/10.5285/a29c5465-b138-234d-e053-6c86abc040b9

Gil MN, Torres AI, Amin O, Esteves JL (2011) Assessment of recent sediment influence in an urban polluted subantarctic coastal ecosystem. Beagle channel (southern Argentina). Mar Pollut Bull 62:201–207

Gill AE (1982) Atmosphere – ocean dynamics. Academic Press, New York, 662 pag

Glembocki NG, Williams GN, Góngora ME, Gagliardini DA, Orensanz JM (2015) Synoptic oceanography of San Jorge gulf (Argentina): a template for Patagonian red shrimp (*Pleoticus muelleri*) spatial dynamics. J Sea Res 95:22–35

Glorioso PD (1987) Temperature distribution related to shelf-sea fronts on the Patagonian shelf. Cont Shelf Res 7:27–34

Glorioso PD, Flather RA (1995) A barotropic model of the currents off SE South America. J Geophys Res 100:13427

Guerrero RA, Acha EM, Framiñan MB, Lasta CA (1997) Physical oceanography of the Río de la Plata Estuary, Argentina. Cont Shelf Res 17:727–742

Guerrero RA, (1998) Oceanografía física del estuario de Río de la Plata y el sistema costero de El Rincón. In: Lasta C (Ed) Resultados de una campaña de evaluación de recursos demersales costeros de la Provincia de Buenos Aires y del litoral uruguayo. Noviembre, 1994. INIDEP, Mar del Plata, Argentina. INIDEP Inf Tec 21:29-54

Guihou K, Piola AR, Palma ED, Chidichimo MP (2020) Dynamical connections between large marine ecosystems of austral South America based on numerical simulations. Ocean Sci 16:271–290

Hallett CS, Hobday AJ, Tweedley JR, Thompson PA, McMahon K, Valesini FJ (2018) Observed and predicted impacts of climate change on the estuaries of South-Western Australia, a Mediterranean climate region. Reg Environ Chang 18:1357–1373

IPCC (2014) Climate Change 2014: Synthesis Report. Contributions of Working Groups I, II and III to the Fifth Assessment Report of the Intergovernmental Panel on Climate Change. Pachauri RK, Meyer LA (eds). IPCC, Geneva, Switzerland, 151 pp.

Isla FI, Isla MF (this volume) Geological changes in coastal areas of Patagonia, Argentina and Chile. In: Helbling EW, Narvarte MA, González RA, Villafañe VE (eds) Global change in Atlantic coastal Patagonian ecosystems. A journey through time. Springer, Cham

Isla F, Bujalesky G, Coronato A (1999) Procesos estuarinos en el canal Beagle, Tierra del Fuego. Rev Asoc Geol Argentina 54:307–318

Jaureguizar AJ, Wiff R, Luz Clara M (2016) Role of the preferred habitat availability for small shark (*Mustelus schmitti*) on the interannual variation of abundance in a large Southwest Atlantic coastal system (El Rincón, 39°–41°S). Aquat Living Resour 29:305

Johnson MS, Meskhidze N, Kiliyanpilakkil VP, Gassó S (2011) Understanding the transport of Patagonian dust and its influence on marine biological activity in the South Atlantic Ocean. Atmos Chem Phys 11:2487–2502

Kopp RE, Horton RM, Little CM, Mitrovica JX, Oppenheimer M, Rasmussen DJ, Strauss BH, Tebaldi C (2014) Probabilistic 21st and 22nd century sea-level projections at a global network of tide-gauge sites. Earth's Future 2:383–406

Krock B, Borel CM, Barrera F, Tillmann U, Fabro E, Almandoz GO, Ferrario M, Garzón Cardona JE, Koch BP, Alonso C, Lara R (2015) Analysis of the hydrographic conditions and cyst beds in the San Jorge gulf, Argentina, that favor dinoflagellate population development including toxigenic species and their toxins. J Mar Syst 148:86–100

Labraga JC (1994) Extreme winds in the Pampa del Castillo Plateau, Patagonia, Argentina, with reference to wind farm settlement. J Appl Meteorol 33:85–95

Lago LS, Saraceno M, Ruiz-Etcheverry LA, Passaro M, Oreiro FA, Donofrio EE, Gonzalez RA (2017) Improved sea surface height from satellite altimetry in coastal zones: a case study in southern Patagonia. IEEE J Sel Top Appl Earth Obs Remote Sens. https://doi.org/10.1109/JSTARS.2017.2694325

Lago LS, Saraceno M, Martos P, Guerrero RA, Piola AR, Paniagua GF, Ferrari R, Artana CI, Provost C (2019) On the wind contribution to the variability of ocean currents over wide continental shelves: a case study on the northern Argentine continental shelf. J Geophys Res Ocean. https://doi.org/10.1029/2019JC015105

Lago LS, Saraceno M, Piola AR, Ruiz-Etcheverry LA (2021) Volume transport variability on the northern Argentine continental shelf from *in situ* and satellite altimetry data. J Geophys Res Ocean. https://doi.org/10.1029/2020JC016813

Lanfredi NW, Pousa JL, D'Onofrio EE (1998) Sea-level rise and related potential hazards on the Argentine coast. J Coast Res 14:47–60

Leyba IM, Solman SA, Saraceno M (2019) Trends in sea surface temperature and air–sea heat fluxes over the South Atlantic Ocean. Clim Dyn. https://doi.org/10.1007/s00382-019-04777-2

Lucas AJ, Guerrero RA, Mianzán HW, Acha EM, Lasta CA (2005) Coastal oceanographic regimes of the Northern Argentine Continental shelf (34-43°S). Estuar Coast Shelf Sci 65:405–420

Marrari M, Piola AR, Valla D, Wilding JG (2016) Trends and variability in extended ocean color time series in the main reproductive area of the Argentine hake, *Merluccius hubbsi* (southwestern Atlantic Ocean). Remote Sens Environ 177:1–12

Marrari M, Piola AR, Valla D (2017) Variability and 20-year trends in satellite-derived surface chlorophyll concentrations in large marine ecosystems around South and Western Central America. Front Mar Sci. https://doi.org/10.3389/fmars.2017.00372

Marshall GJ (2003) Trends in the Southern Annular Mode from observations and reanalyses. J Clim 16:4134–4143

Marshall GJ, Orr A, van Lipzig NPM, King JC (2006) The impact of a changing Southern Hemisphere Annular Mode on Antarctic Peninsula summer temperatures. J Clim 19:5388–5404

Martin J, Colloca C, Diodato S, Malits A, Kreps G (2016) Variabilidad espacio-temporal de las concentraciones de oxígeno disuelto en Bahía Ushuaia y Canal Beagle (Tierra del Fuego). Nat Patagonica 8:193

Matano RP, Palma ED (2008) On the upwelling of downwelling currents. J Phys Oceanogr 38:2482–2500

Matano R, Palma E (2018) Seasonal variability of the oceanic circulation in the gulf of San Jorge, Argentina. Oceanography. https://doi.org/10.5670/oceanog.2018.402

Matano RP, Palma ED, Piola AR (2010) The influence of the Brazil and Malvinas currents on the southwestern Atlantic shelf circulation. Ocean Sci 6:983–995

Mellor GL, Yamada T (1982) Development of a turbulence closure model for geophysical fluid problems. Rev Geophys 20:851–875

Melo XF, Martín J, Kerdel L, Bourrin F, Colloca CB, Menniti C, de Madron XD (2020) Particle dynamics in Ushuaia Bay (Tierra del Fuego)-potential effect on dissolved oxygen depletion. Water (Switzerland). https://doi.org/10.3390/w12020324

Moreira D, Simionato CG, Dragani WC, Nuñez MN (2009) Tidal and residual currents observations at the San Matías and San José gulfs, northern Patagonia. Argentina J Coast Res 254:957–968

Moreira D, Simionato CG, Dragani W (2011) Modeling ocean tides and their energetics in the North Patagonia gulfs of Argentina. J Coast Res. https://doi.org/10.2112/JCOASTRES-D-09-00055.1

Narvarte MA, Avaca MS, de la Barra P, Góngora ME, Jaureguízar AJ, Ocampo Reinaldo M, Romero MA, Storero LP, Svendsen GM, Tapella F, Zaidman P, González RA (this volume) The Patagonian fisheries over time: facts and lessons to be learned to face global change. In: Helbling EW, Narvarte MA, González RA, Villafañe VE (eds) Global change in Atlantic coastal Patagonian ecosystems. A journey through time. Springer, Cham

Oppenheimer M, Glavovic BC, Hinkel J (2019) Sea Level Rise and Implications for Low-Lying Islands, Coasts and Communities. In: Pörtner HO et al (eds) IPCC Special Report on the Ocean and Cryosphere in a Changing Climate.

Palma ED (2002) Tides and tidal energy in Valdés Península (Argentina). Revista geofísica 56:31.
Palma ED, Matano RP (2012) A numerical study of the Magellan Plume. J Geophys Res Ocean. https://doi.org/10.1029/2011JC007750
Palma ED, Matano RP, Piola AR (2004) A numerical study of the southwestern Atlantic shelf circulation: barotropic response to tidal and wind forcing. J Geophys Res C Ocean 109:C8. https://doi.org/10.1029/2004JC002315
Palma ED, Matano RP, Piola AR (2008) A numerical study of the southwestern Atlantic shelf circulation: stratified ocean response to local and offshore forcing. J Geophys Res Ocean. https://doi.org/10.1029/2007JC004720
Palma ED, Matano RP, Tonini MH, Martos P, Combes V (2020) Dynamical analysis of the oceanic circulation in the Gulf of San Jorge, Argentina. J Mar Syst, 203. https://doi.org/10.1016/j.jmarsys.2019.103261
Panella S, Michelato A, Perdicaro R, Magazzu G, Decembrini F, Scarazzato P (1991) A preliminary contribution to understanding the hydrological characteristics of the strait of Magellan: austral spring 1989. Boll Oceanol Teor Appl 9:107–126
Paparazzo FE, Crespi-Abril AC, Gonçalves RJ, Barbieri ES, Gracia Villalobos LL, Solís ME, Soria G (2018) Patagonian dust as a source of macronutrients in the Southwest Atlantic Ocean. Oceanography 31:33–39
Penland C, Sun D-Z, Capotondi A, Vimont DJ (2013) A brief introduction to El Niño and La Niña. Clim Dyn Why Does Clim Vary. https://doi.org/10.1029/2008GM000846
Pérez I, Alonso G, Pescio A, Dragani W, Codignotto J (2017) Longshore wave energy flux: variability and trends in the southern coast of Buenos Aires, Argentina. Reg Stud Mar Sci 16:116–123
Perrette M, Landerer F, Riva R, Frieler K, Meinshausen M (2013) A scaling approach to project regional sea level rise and its uncertainties. Earth Syst Dynam 4:11–29
Pessacg N, Blázquez J, Lancelotti J, Solman S (this volume) Climate changes in coastal areas of Patagonia: observed trends and future projections. In: Helbling EW, Narvarte MA, González RA, Villafañe VE (eds) Global change in Atlantic coastal Patagonian ecosystems. A journey through time. Springer, Cham
Piola AP, Scasso LM (1988) Circulación en el golfo San Matías. Geoacta 15:33–51
Piola AR, Matano RP, Palma ED, Möller OO, Campos EJD (2005) The influence of the Plata river discharge on the western South Atlantic shelf. Geophys Res Lett 32:1–4
Piola AR, Martínez Avellaneda N, Guerrero RA, Jardón FP, Palma ED, Romero SI (2010) Malvinas-slope water intrusions on the northern Patagonia continental shelf. Ocean Sci. https://doi.org/10.5194/os-6-345-2010
Piola AR, Palma ED, Bianchi AA, Castro BM, Dottori M, Guerrero RA, Marrari M, Matano RP, Möller OO, Saraceno M (2018) Physical oceanography of the SW Atlantic shelf: a review. In: Hoffmeyer MS, Sabatini ME, Brandini FP, Calliari DL, Santinelli NH (eds) Plankton ecology of the southwestern Atlantic: from the subtropical to the Subantarctic realm. Springer, Cham, pp 37–56
Pisoni JP (2012) Los sistemas frontales y la circulación en las inmediaciones de los Golfos Norpatagónicos. Doctoral Thesis, Universidad de Buenos Aires, 197 pp.
Pisoni JP, Rivas AL, Piola AR (2014) Satellite remote sensing reveals coastal upwelling events in the San Matías Gulf-Northern Patagonia. Remote Sens Environ 152:270–278
Pisoni JP, Rivas AL, Piola AR (2015) On the variability of tidal fronts on a macrotidal continental shelf, northern Patagonia, Argentina. Deep Sea Res Part II Top Stud Oceanogr 119:61–68
Pisoni JP, Rivas AL, Tonini MH (2020) Coastal upwelling in the San Jorge gulf (southwestern Atlantic) from remote sensing, modelling and hydrographic data. Estuar Coast Shelf Sci 245:106919
Poli L, Artana C, Provost C, Sirven J, Sennéchael N, Cuypers Y, Lellouche J-M (2020) Anatomy of subinertial waves along the Patagonian shelf break in a 1/12° global operational model. J Geophys Res Ocean. https://doi.org/10.1029/2020JC016549
Rabassa J (2008) Late Cenozoic glaciations in Patagonia and Tierra del Fuego. Dev Quat Sci. https://doi.org/10.1016/S1571-0866(07)10008-7

Rabassa J, Clapperton CM (1990) Quaternary glaciations of the southern Andes. Quat Sci Rev 9:153–174

Reiter ML, Luz Clara Tejedor M, Moreira D (2019) Distribución de temperatura y salinidad en la región de El Rincón a partir de observaciones in situ durante el período 1978–2018. XVIII Congreso Latinoamericano de Ciencias del Mar, 4 y 8 de noviembre de 2019, Mar del Plata, Argentina

Reynolds RW, Smith TM, Liu C, Chelton DB, Casey KS, Schlax MG (2007) Daily high-resolution-blended analyses for sea surface temperature. J Clim 20:5473–5496

Rhein M, Rintoul SR, Aoki S, Campos E, Chambers D, Feely RA, Gulev S, Johnson GC, Josey SA, Kostianoy A, Mauritzen C, Roemmich D, Talley LD, Wang F (2013) Observations: Ocean. In: Climate Change 2013: The Physical Science Basis. Contribution of Working Group I to the Fifth Assessment Report of the Intergovernmental Panel on Climate Change, Stocker TF et al. (eds). Cambridge University Press, Cambridge, United Kingdom and New York, NY, USA, pp 255–316. https://doi.org/10.1017/CBO9781107415324.010

Rivas A (1990) Heat balance and annual variation of mean temperature in the North-Patagonian gulfs. Oceanol Acta 13:265–272

Rivas AL (1997) Current-meter observations in the Argentine continental shelf. Cont Shelf Res 17:391–406

Rivas AL, Beier EJ (1990) Temperature and salinity fields in the northpatagonic gulfs. Ocean Acta 13:15–20

Rivas AL, Pisoni JP (2010) Identification, characteristics and seasonal evolution of surface thermal fronts in the Argentinean continental shelf. J Mar Syst 79:134–143

Rodrigues KA, Jaureguizar AJ, Guerrero RA (2013) Environmental factors that define the spawning and nursery areas for *Percophis brasiliensis* (Teleostei: Percophididae) in a multispecific reproductive coastal zone, El Rincón (39°–41°S), Argentina. Hydrobiologia 709:1–10

Romero SI, Piola AR, Charo M, Eiras Garcia CA (2006) Chlorophyll – a variability off Patagonia based on SeaWiFS data. J Geophys Res Ocean. https://doi.org/10.1029/2005JC003244

Ruiz Etcheverry LA, Saraceno M, Piola AR, Valladeau G, Möller OO (2015) A comparison of the annual cycle of sea level in coastal areas from gridded satellite altimetry and tide gauges. Cont Shelf Res 92:87–97

Ruiz Etcheverry LA, Saraceno M, Piola AR, Strub PT (2016) Sea level anomaly on the Patagonian continental shelf: trends, annual patterns and geostrophic flows. J Geophys Res Ocean. https://doi.org/10.1002/2015JC011265

Ruiz-Etcheverry LA, Saraceno M (2020) Sea level trend and fronts in the South Atlantic Ocean. Geoscience. https://doi.org/10.3390/geosciences10060218

Sabatini M, Martos P (2002) Mesozooplankton features in a frontal area off northern Patagonia (Argentina) during spring 1995 and 1998. Sci Mar 66:215–232

Sabatini ME, Reta R, Lutz VA, Segura V, Daponte C (2016) Influence of oceanographic features on the spatial and seasonal patterns of mesozooplankton in the southern Patagonian shelf (Argentina, SW Atlantic). J Mar Syst 157:20–38

Santamaria-Aguilar S, Schuerch M, Vafeidis AT, Carretero SC (2017) Long-term trends and variability of water levels and tides in Buenos Aires and Mar del Plata, Argentina. Front Mar Sci 4:380

Saraceno M, Provost C, Piola AR, Bava J, Gagliardini A (2004) Brazil Malvinas Frontal System as seen from 9 years of advanced very high resolution radiometer data. J Geophys Res C Ocean 109. https://doi.org/10.1029/2003JC002127

Saraceno M, Provost C, Piola AR (2005) On the relationship between satellite-retrieved surface temperature fronts and chlorophyll a in the western South Atlantic. J Geophys Res Ocean 110:1–16

Saraceno M, D'Onofrio EE, Fiore ME, Grismeyer WH (2010) Tide model comparison over the southwestern Atlantic shelf. Cont Shelf Res 30:1865–1875

Saraceno M, Simionato CG, Ruiz-Etcheverry LA (2014) Sea surface height trend and variability at seasonal and interannual time scales in the southeastern South American continental shelf between 27°S and 40°S. Cont Shelf Res 91:82–94

Saraceno M, Tonini MH, Williams GN, Aubone N, Olascoaga MJ, Beron-Vera FJ, Gonzalez R, Soria M, Saad JF, Svendsen G (2020) On the complementary information provided by satellite images, Lagrangian drifters, and a regional numerical model: a case study in the San Matías Gulf, Argentina. Remote Sens Earth Syst Sci. https://doi.org/10.1007/s41976-020-00039-6

Scasso LM, Piola AP (1988) Intercambio neto de agua entre el mar y la atmósfera en el golfo San Matías. Geoacta 15:13–31

Schloss I, Ferreyra G, Ferrario M, Almandoz G, Codina R, Bianchi A, Balestrini C, Ochoa H, Ruiz Pino D, Poisson A (2007) Role of plankton communities in sea-air variations in pCO_2 in the SW Atlantic Ocean. Mar Ecol Prog Ser 332:93–106

Shchepetkin AF, McWilliams JC (2005) The regional oceanic modeling system (ROMS): a split-explicit, free-surface, topography-following-coordinate oceanic model. Ocean Model 9:347–404

SHN (2018) Tablas de Marea. Servicio de Hidrografía Naval. Ministerio de Defensa, Argentina.

Sievers AH, Silva N, (2008) Water masses and circulation in austral Chilean channels and fjords. In: Silva N, Palma S, (eds), Progress in the Oceanographic Knowledge of Chilean Inner Waters, from Puerto Montt to Cape Horn. Comité Oceanográfico Nacional – Pontificia Universidad Católica de Valparaíso, Valparaíso, Chile, pp. 53–58

Slangen ABA, Carson M, Katsman CA, van de Wal RSW, Köhl A, Vermeersen LLA, Stammer D (2014) Projecting twenty-first century regional sea-level changes. Clim Chang 124:317–332

St-Onge G, Ferreyra G (2018) Introduction to the special issue on the gulf of San Jorge (Patagonia, Argentina). Oceanography 31:14–15

Strelin J, Iturraspe R (2007) Recent evolution and mass balance of Cordón Martial glaciers, cordillera Fueguina Oriental. Glob Planet Change 59:17–26

Strub PT, James C, Combes V, Matano RP, Piola AR, Palma ED, Saraceno M, Guerrero RA, Fenco H, Ruiz-Etcheverry LA (2015) Altimeter-derived seasonal circulation on the Southwest Atlantic shelf: 27°-43°S. J Geophys Res Ocean 120:3391–3418

Strub PT, James C, Montecino V, Rutllant JA, Blanco JL (2019) Ocean circulation along the southern Chile transition region (38°–46°S): mean, seasonal and interannual variability, with a focus on 2014–2016. Prog Oceanogr 172:159–198

Sylwan C (2001) Geología de la cuenca del golfo San Jorge, Argentina. J Iber Geol 27:123–157

Temperoni B, Massa AE, Derisio C, Martos P, Berghoff C, Viñas MD (2018) Effect of nursery ground variability on condition of age 0+ year *Merluccius hubbsi*. J Fish Biol 93:1090–1101

Thompson PR, Mitchum GT (2014) Coherent sea level variability on the North Atlantic western boundary. J Geophys Res Ocean 119:5676–5689

Thompson DWJ, Solomon S, Kushner PJ, England MH, Grise KM, Karoly DJ (2011) Signatures of the Antarctic ozone hole in Southern Hemisphere surface climate change. Nat Geosci 4:741–749

Tonini MH, Palma ED (2017) Tidal dynamics on the North Patagonian Argentinean gulfs. Estuar Coast Shelf Sci 189:115–130. https://doi.org/10.1016/j.ecss.2017.02.026

Tonini MH, Palma ED, Rivas AL (2006) Modelo de alta resolución de los golfos Patagónicos. Mecánica Comput 25:1441–1460

Tonini MH, Palma ED, Piola AR (2013) A numerical study of gyres, thermal fronts and seasonal circulation in austral semi-enclosed gulfs. Cont Shelf Res 65:97–110

Torres A, Paparazzo F, Williams G, Rivas A, Solis M, Esteves J (2018) Dynamics of macronutrients in the San Jorge gulf during spring and summer. Oceanography 31:25–32

Villafañe VE, Cabrerizo MJ, Carrillo P, Hernando MP, Medina-Sánchez JM, Narvarte MA, Saad JF, Valiñas MS, Helbling EW (this volume) Global change effects on plankton from Atlantic Patagonian coastal waters: role of interacting drivers. In: Helbling EW, Narvarte MA, González RA, Villafañe VE (eds) Global change in Atlantic coastal Patagonian ecosystems. A journey through time. Springer, Cham

Wörner S, Dragani WC, Echevarria ER, Carrasco M, Barón PJ (2019) An estimation of the possible migration path of the Pacific oyster (*Crassostrea gigas*) along the northern coast of Patagonia. Estuar Coasts 42:806–821